

Continued Fractions and the Partially Asymmetric Exclusion Process

R. A. Blythe

SUPA, School of Physics and Astronomy, University of Edinburgh, Mayfield Road,
Edinburgh EH9 3JZ

W. Janke

Institut für Theoretische Physik and Centre for Theoretical Sciences (NTZ),
Universität Leipzig, Postfach 100 920, 04009 Leipzig, Germany

D. A. Johnston

Department of Mathematics and the Maxwell Institute for Mathematical Sciences,
Heriot-Watt University, Riccarton, Edinburgh EH14 4AS, Scotland

R. Kenna

Applied Mathematics Research Centre, Coventry University, Coventry, CV1 5FB,
England

Abstract. We note that a tridiagonal matrix representation of the algebra of the partially asymmetric exclusion process (PASEP) lends itself to interpretation as the transfer matrix for weighted Motzkin lattice paths. A continued fraction (“J-Fraction”) representation of the lattice path generating function is particularly well suited to discussing the PASEP, for which the paths have height dependent weights. We show that this not only allows a succinct derivation of the normalisation and correlation lengths of the PASEP, but also reveals how finite-dimensional representations of the PASEP algebra, valid only along special lines in the phase diagram, relate to the general solution that requires an infinite-dimensional representation.

PACS numbers: 05.40.-a, 05.70.Fh, 02.50.Ey

1. Introduction

Although the asymmetric exclusion process (ASEP)—a model in which hard-core particles hop in a preferred direction along a one-dimensional lattice—has been reinvented in various different guises over the years, it is only relatively recently that exact solutions for the steady state(s) of the model have been available. The solution of the ASEP with open boundary conditions in [1] using a matrix product ansatz was a landmark in the study of driven diffusive systems.

As discussed in a recent review of the matrix product approach to solving for the steady state of nonequilibrium Markov processes [2], there are a range of different methods for analysing the thermodynamic phase behaviour of the simplest versions of the ASEP. By contrast, more general models—collectively known as the partially asymmetric exclusion process (PASEP)—that admit particles to hop in both directions in the bulk, and even more generally to enter and exit at both left and right boundaries, have so far been studied only through a diagonalisation of the matrices appearing in the formalism [3–5]. In this work, we extend a technique that previously admitted an extremely quick derivation of the ASEP phase behaviour under various updating schemes [6, 7] to these more general models.

The idea is to consider the behaviour of a “grand-canonical partition function” for the model. More precisely, we examine the generating function of the normalization of the nonequilibrium steady-state distribution over an ensemble of different lattice lengths whose mean is controlled by a fugacity. The thermodynamic phase behaviour can then be read off from the singularities of this generating function. Whilst obtaining this generating function is straightforward for the ASEP [6, 7], a convenient closed form for the PASEP has remained elusive.

Our aim here is to demonstrate that a representation of the generating function that allows the thermodynamic phase behaviour to be determined with relative ease takes the form of an infinite continued fraction. This we arrive at through an interpretation of the PASEP normalization as the (equilibrium) partition function of lattice paths, which we discuss in Section 3 after recalling the model definition and its basic properties. In Section 4 we show how to analyse the singularities embedded in the continued fraction representation. The results we obtain are, of course, equivalent to those obtained within other approaches [3–5]. However, given that continued fractions are not frequently encountered in statistical mechanical contexts, we feel there is some value in using the PASEP as an illustrative example of how to handle them.

We find that the analysis is intimately related to an approach based on finite-dimensional matrix representations [8,9], exact along special lines in the phase diagram, and that the continued fraction shows how these particular solutions and the general solution are related. We further show that the continued-fraction approach extends to the most general version of the PASEP, solved in [5], and that one can access both currents and correlation lengths through it. Finally, we return to the lattice path picture to elucidate the equilibrium counterpart of a nonequilibrium phase transition identified

in [4] that occurs when the bias on bulk hop rates opposes that imposed by the boundary conditions.

2. Model Definition and Basic Properties

The dynamics of the PASEP take place on a finite one-dimensional lattice with open boundaries. In its simplest form, the microscopic dynamics of the PASEP are specified by four rates, one of which can be set to unity by an overall scaling. For a rate λ associated with a particular event, the probability that the event happens in an infinitesimal time interval Δt is $\lambda\Delta t$. Moves that would lead to two particles occupying a single lattice site at any one time are prohibited due to the hard-core repulsion between them.

In the PASEP particles are inserted onto the left boundary site (when empty) at a rate α and removed from the right boundary site at a rate β , see figure 1. Once on the lattice a particle hops by one site to the right at rate 1 or by one site to the left at a rate q when sites are available (i.e. empty). It is possible to expand this set of moves to allow particles to enter at the right at a rate δ and exit at the left at a rate γ , while still retaining the solvability of the model [5].

In all the models we consider we want to calculate Z , which normalises the statistical weight, $f(\mathcal{C})$, of a lattice configuration, \mathcal{C} , in the steady state. This is given by

$$Z = \sum_{\mathcal{C}} f(\mathcal{C}) , \quad (2.1)$$

so the normalized probability of being in state \mathcal{C} is $P(\mathcal{C}) = f(\mathcal{C})/Z$.

The weights themselves are obtained through the stationarity condition on the transition rates $W(\mathcal{C} \rightarrow \mathcal{C}')$,

$$\sum_{\mathcal{C}' \neq \mathcal{C}} [f(\mathcal{C}')W(\mathcal{C}' \rightarrow \mathcal{C}) - f(\mathcal{C})W(\mathcal{C} \rightarrow \mathcal{C}')] = 0 , \quad (2.2)$$

where $W(\mathcal{C} \rightarrow \mathcal{C}')$ is the probability of making the transition from configuration \mathcal{C} to \mathcal{C}' in a single timestep. This is less restrictive than the detailed balance condition for equilibrium states, which is obtained when the sum in equation (2.2) vanishes term by term.

The solution of the ASEP in [1] and the PASEP in [3–5] made use of a matrix product ansatz [2]. In this the steady-state probability $P(\mathcal{C})$ of a configuration of particles \mathcal{C} on a chain of length N is represented by an ordered product of matrices $X_1 X_2 \dots X_N$ where $X_i = D$ if site i is occupied and $X_i = E$ if it is empty. We expect

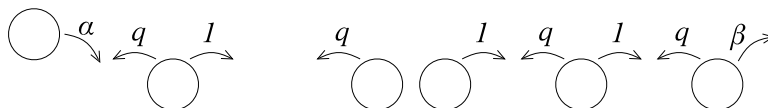


Figure 1. Typical particle configuration and allowed moves in the PASEP model.

$P(\mathcal{C})$ to be a function of both the number and position of particles on the lattice, which suggests the choice of non-commuting objects, matrices, for the ansatz. To obtain a scalar probability value from this matrix product it is sandwiched between two vectors $\langle W|$ and $|V\rangle$:

$$P(\mathcal{C}) = \frac{\langle W|X_1X_2\dots X_N|V\rangle}{Z_N} . \quad (2.3)$$

The factor Z_N is included to ensure that $P(\mathcal{C})$ is properly normalised. This latter quantity plays the role of a partition function in equilibrium problems

$$Z_N = \langle W|(D + E)^N|V\rangle = \langle W|C^N|V\rangle , \quad (2.4)$$

where we have defined $C = D + E$. Indeed, we shall see in what follows that Z_N is the partition function for an equivalent two-dimensional lattice path problem.

The algebraic properties of the matrices D and E can be deduced from the master equation for the dynamics of the ASEP, PASEP and various other related models [2]. For the variant of the PASEP discussed above, sufficient conditions for equation (2.3) to hold are

$$DE - qED = D + E , \quad (2.5)$$

$$\alpha\langle W|E = \langle W| , \quad (2.6)$$

$$\beta D|V\rangle = |V\rangle . \quad (2.7)$$

These relations allow one to calculate Z_N and other quantities of physical interest by a range of methods, such as “normal-ordering” of the matrices, or through use of explicit representations [2].

In this work, we focus on an approach based around the generating function of Z_N , namely $\mathcal{Z}(z) = \sum_N Z_N z^N$, which can be thought of as a “grand-canonical” normalization. As is well known [10], the large- N form of the “canonical” normalization (Z_N) can be determined from the dominant singularity z_{cr} of $\mathcal{Z}(z)$. Typically, $Z_N \sim z_{cr}^{-N} N^{-\nu}$ where the exponent $\nu \geq 0$ depends on the nature of the singularity. Then, by defining a “reduced free energy” f via

$$f = - \lim_{N \rightarrow \infty} \frac{1}{N} \ln Z_N , \quad (2.8)$$

we find $f = \ln z_{cr}$. Nonanalyticities in f can then be associated with phase transitions in the physical system [2, 6, 7, 11].

For orientation, let us recall the results for the ASEP, which has $q = 0$. The canonical normalization can be shown by direct matrix reordering [1] to be

$$Z_N = \sum_{p=1}^N \frac{p(2N-1-p)! (1/\beta)^{p+1} - (1/\alpha)^{p+1}}{N!(N-p)! (1/\beta) - (1/\alpha)} . \quad (2.9)$$

Performing the summation [6] gives the grand canonical normalization

$$\mathcal{Z}(z) = \frac{\alpha\beta}{(\alpha - x(z))(\beta - x(z))} , \quad (2.10)$$

where $x(z) = (1 - \sqrt{1 - 4z})/2$.

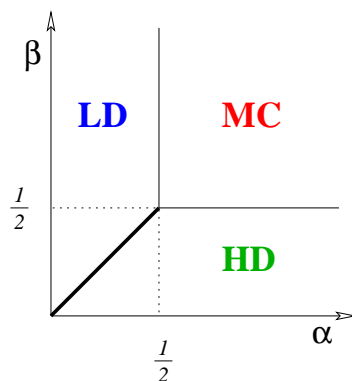


Figure 2. The phase diagram of the ASEP. Here HD, LD and MC denote the high-density, low-density and maximal-current phases, respectively.

This function has a pole at $x(z) = \alpha$ when $\alpha < \frac{1}{2}$ and similarly at $x(z) = \beta$ when $\beta < \frac{1}{2}$. These correspond to $z_{cr} = \alpha(1 - \alpha)$ and $z_{cr} = \beta(1 - \beta)$. When neither of these poles contribute, all that remains is the square-root singularity at $z_{cr} = \frac{1}{4}$. This allows one to very quickly establish the behaviour of the reduced free energy as a function of α and β :

$$f = \begin{cases} \ln \left[\frac{1}{4} \right] & \text{for } \alpha, \beta > 1/2 \\ \ln [\alpha(1 - \alpha)] & \text{for } \beta > \alpha, \alpha < 1/2 \\ \ln [\beta(1 - \beta)] & \text{for } \alpha > \beta, \beta < 1/2 \end{cases} . \quad (2.11)$$

It turns out that for the ASEP, z_{cr} corresponds to the particle current, and $x(z_{cr})$ the bulk density in the thermodynamic limit. Hence, the phase diagram for the model, Figure 2, is quickly recovered using this generating-function (or grand-canonical) analysis. Further details of these methods as applied to the ASEP can be found in [2,6,7]. In the remainder of this work, we show how to elicit the structure of the grand-canonical normalization of the PASEP, where direct summation of the canonical normalization, given explicitly in [4], does not lead to a compact expression like (2.10).

3. Explicit Matrix Representation and Lattice Path Interpretation

A useful route to the grand-canonical normalization for the PASEP is via the generating function for an ensemble of lattice paths, which in turn can be read off from an explicit representation of the matrices and vectors appearing in the equations (2.5), (2.6) and (2.7) that define the matrix algebra. A number of representations are known, see [1–3,5]; the one that is of use here is that for which the vectors $\langle W|$ and $|V\rangle$ have nonzero entries only in their first element:

$$\langle W_q| = \langle W| = h_0^{1/2}(1, 0, 0, \dots) \quad |V_q\rangle = |V\rangle = h_0^{1/2}(1, 0, 0, \dots)^T, \quad (3.12)$$

where h_0 is a constant to be given shortly. One can verify that, with this choice of boundary vectors, the following tridiagonal representations of D and E satisfy (2.5),

(2.6) and (2.7):

$$D_q = \frac{1}{1-q} \begin{pmatrix} 1 + \tilde{\beta} & \sqrt{c_1} & 0 & \cdots \\ 0 & 1 + \tilde{\beta}q & \sqrt{c_2} & \\ 0 & 0 & 1 + \tilde{\beta}q^2 & \ddots \\ \vdots & & \ddots & \ddots \end{pmatrix},$$

$$E_q = \frac{1}{1-q} \begin{pmatrix} 1 + \tilde{\alpha} & 0 & 0 & \cdots \\ \sqrt{c_1} & 1 + \tilde{\alpha}q & 0 & \\ 0 & \sqrt{c_2} & 1 + \tilde{\alpha}q^2 & \ddots \\ \vdots & & \ddots & \ddots \end{pmatrix}. \quad (3.13)$$

The various parameters that appear are

$$\tilde{\alpha} = \frac{1-q}{\alpha} - 1, \quad (3.14)$$

$$\tilde{\beta} = \frac{1-q}{\beta} - 1, \quad (3.15)$$

$$c_n = (1-q^n)(1 - \tilde{\alpha}\tilde{\beta}q^{n-1}), \quad (3.16)$$

$$h_0 = \frac{1}{(\tilde{\alpha}\tilde{\beta}; q)_\infty} = \sum_{n=0}^{\infty} \frac{(\tilde{\alpha}\tilde{\beta})^n}{(q; q)_n} = \langle W|V \rangle, \quad (3.17)$$

in which we have used the standard notation for (shifted) q -factorials

$$(a; q)_n = \prod_{j=0}^{n-1} (1 - aq^j),$$

$$(a; q)_0 = 1,$$

$$(a, b, \dots, c; q)_n = (a; q)_n (b; q)_n \cdots (c; q)_n. \quad (3.18)$$

There are various ways to arrive at an interpretation in terms of lattice paths from a matrix representation. One was suggested by Brak and Essam [12, 13], who used the fact that $D + E = DE$ for the ASEP to interpret the D and E as odd-even and even-odd height transfer matrices separately. In later works [6, 7], the path interpretation was inferred from the grand-canonical normalization once this had been obtained by another means. Here, we shall take the most direct approach, which is to associate a height $n \geq 0$ above the origin with the vector $|n\rangle = (0 \ 0 \ \cdots \ 0 \ 1 \ 0 \ \cdots)^T$ (i.e., n is the number of zero entries that appear before the single nonzero entry). We then interpret $\langle m|X|n\rangle$, where X is some combination of D and E matrices, as the weight of paths connecting a point at height n to another point at height m .

Of particular importance is the matrix $X = C^N$, which appears in Eq. (2.4) for the normalization. From the above expressions we have that

$$C_q = D_q + E_q = \frac{1}{1-q} \begin{pmatrix} 2 + \tilde{\alpha} + \tilde{\beta} & \sqrt{c_1} & 0 & \cdots \\ \sqrt{c_1} & 2 + (\tilde{\alpha} + \tilde{\beta})q & \sqrt{c_2} & \\ 0 & \sqrt{c_2} & 2 + (\tilde{\alpha} + \tilde{\beta})q^2 & \ddots \\ \vdots & & \ddots & \ddots \end{pmatrix}. \quad (3.19)$$

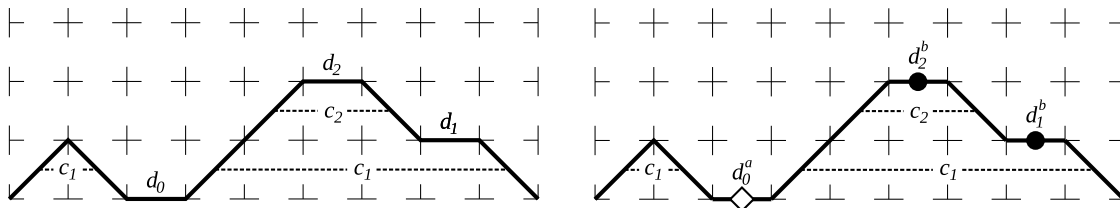


Figure 3. Two Motzkin path transliterations of the tridiagonal matrix representation of the PASEP matrices. In both cases, up-step down-step pairs contribute a weight c_n , where n is the height above the origin of the upper end of the steps. In the left-hand figure, there is a single type of horizontal step that contributes a weight d_n , where n is the height of the segment above the origin. The right-hand figure shows an equivalent interpretation, in which there are two types of horizontal steps, shown with diamonds and circles at their midpoints. These contribute weights d_n^a and d_n^b , respectively.

The matrix element $\langle m|C^N|n\rangle$ then gives the combined weight of paths that begin at height m , end at height n and contain N steps, each of which may raise or lower the height by one unit, or leave the height unchanged. Since the height is a nonnegative quantity, $n \geq 0$, these paths may never descend beneath the origin. Additionally, since $\langle W| \propto \langle 0|$ and $|V\rangle \propto |0\rangle$, the paths that contribute to Z_N begin and end at the origin. Paths with these properties are known as *Motzkin paths*.

The weight of various path components can now be obtained by inspecting the form of C_q . For the path to begin and end at the origin, every up-step must be accompanied by a down-step; each up-step down-step pair connecting height $n-1$ to height n contributes a weight c_n to the path. Each horizontal step at height n contributes a weight $d_n = 2 + (\tilde{\alpha} + \tilde{\beta})q^n$ to the path. An alternative interpretation has two types (or “colours”) of horizontal path segments, one of which contributes a weight $d_n^a = 1 + \tilde{\alpha}q^n$ and the other $d_n^b = 1 + \tilde{\beta}q^n$. See figure 3. To arrive at the canonical normalization Z_N , we sum over all paths of length N , and multiply by the factor $h_0/(1-q)^N$. The grand-canonical normalization is constructed by summing paths of all lengths, weighting each segment by z , and finally multiplying by h_0 . In the next section, we shall see an equivalent recursive construction which can be expressed as a continued fraction.

As a check of the path representation one can compare the expression for Z_N which emerges from directly evaluating the matrix product expression for the stationary state,

$$Z_N = \langle W|V\rangle \left(\frac{1}{1-q}\right)^N \sum_{n=0}^N R_{N,n}(q) B_n(\tilde{\alpha}, \tilde{\beta}; q), \quad (3.20)$$

where

$$R_{N,n}(q) = \sum_{k=0}^{\lfloor \frac{N-n}{2} \rfloor} (-1)^k \left[\binom{2N}{N-n-2k} - \binom{2N}{N-n-2k-2} \right] q^{\binom{k+1}{2}} \begin{bmatrix} n+k \\ k \end{bmatrix}, \quad (3.21)$$

and

$$B_n(\tilde{\alpha}, \tilde{\beta}; q) = \sum_{k=0}^n \begin{bmatrix} n \\ k \end{bmatrix} \tilde{\alpha}^{n-k} \tilde{\beta}^k, \quad (3.22)$$

with the weights which emerge from the contributing paths at low orders. In the above we have used the standard notation for the q -binomial coefficient

$$\begin{bmatrix} n \\ k \end{bmatrix} = \frac{(q; q)_n}{(q; q)_{n-k}(q; q)_k}. \quad (3.23)$$

For instance, taking the simple case of Z_2 a direct calculation using the above formulae gives

$$Z_2 = \frac{5 - q + \tilde{\alpha}^2 + \tilde{\alpha}\tilde{\beta} + \tilde{\beta}^2 + q\tilde{\alpha}\tilde{\beta} + 4\tilde{\alpha} + 4\tilde{\beta}}{(1 - q)^2}, \quad (3.24)$$

where we have dropped the overall normalization $\langle W|V \rangle$. The $(1 - q)^2$ denominator disappears when this is written in terms of the original rate parameters α and β ,

$$Z_2 = \frac{\alpha\beta q + \alpha^2 + \beta^2\alpha + \alpha\beta + \alpha^2\beta + \beta^2}{\alpha^2\beta^2}. \quad (3.25)$$

The expression for Z_2 in (3.24) can be seen to be the sum of weights for an up/down step pair from level 0 to 1, given by $(1 - q)(1 - \tilde{\alpha}\tilde{\beta})/(1 - q)^2$ and all four possible combinations of two horizontal steps at level zero of either ‘‘colour’’, given by $(2 + \tilde{\alpha} + \tilde{\beta})(2 + \tilde{\alpha} + \tilde{\beta})/(1 - q)^2$ (where we have again dropped the overall normalization $\langle W|V \rangle$). While the diagrammatics becomes increasingly complicated for larger Z_N , the principle remains the same.

4. The Continued Fraction Representation of the Path Generating Function

Despite the availability of an exact expression for the canonical normalization, Eq. (3.20) from [4], we have not been able to find a convenient expression for its grand-canonical counterpart due to the q -dependence of the PASEP weights. A more fruitful route is to represent the lattice-path generating function as a continued fraction, a procedure first expounded by Flajolet [14]. As we now show, this representation can be read off more-or-less directly from the matrix representation (3.19), and the form that emerges is particularly well adapted to discussion of the PASEP.

First, for convenience, we subsume the prefactor $1/(1 - q)$ appearing in (3.19) into the parameters

$$\begin{aligned} \tilde{d}_n &= \frac{2 + (\tilde{\alpha} + \tilde{\beta})q^n}{1 - q}, \\ \tilde{c}_n &= \frac{(1 - q^n)(1 - \tilde{\alpha}\tilde{\beta}q^{n-1})}{(1 - q)^2}, \end{aligned} \quad (4.26)$$

so that then

$$C_q = \begin{pmatrix} \tilde{d}_0 & \sqrt{\tilde{c}_1} & 0 & \cdots \\ \sqrt{\tilde{c}_1} & \tilde{d}_1 & \sqrt{\tilde{c}_2} & \\ 0 & \sqrt{\tilde{c}_2} & \tilde{d}_2 & \ddots \\ \vdots & & \ddots & \ddots \end{pmatrix}. \quad (4.27)$$

In the lattice-path language, this means that horizontal steps at height n are weighted by \tilde{d}_n and up-down step pairs between heights n and $n + 1$ are weighted by \tilde{c}_n .

Let now $\mathcal{M}_n(z)$ be the generating function of weighted Motzkin paths that start and end at height n , never go below this height, and have their lengths $N \geq 0$ counted by powers of z . That is, the coefficient of z^N in $\mathcal{M}_n(z)$ is the weight of such paths of length N . The grand-canonical normalization for the PASEP is then given by $\mathcal{Z}(z) = h_0 \mathcal{M}_0(z)$. Let us suppose that $\mathcal{M}_{n+1}(z)$ is known for some $n \geq 0$. Then, we can construct $\mathcal{M}_n(z)$ by concatenating contiguous components of two types: (i) sequences of horizontal segments of arbitrary (possibly zero) length at height n ; and (ii) Motzkin paths starting at height $n + 1$ enclosed by an up-down pair. Denoting these components schematically as $_$ and $\swarrow \mathcal{M}_{n+1} \searrow$ respectively, we can write the recursion

$$\mathcal{M}_n = _ + _ \swarrow \mathcal{M}_{n+1} \searrow _ + _ \swarrow \mathcal{M}_{n+1} \searrow _ \swarrow \mathcal{M}_{n+1} \searrow _ + \cdots \quad (4.28)$$

$$= _ (1 + [\swarrow \mathcal{M}_{n+1} \searrow] + [\swarrow \mathcal{M}_{n+1} \searrow]^2 + \cdots) \quad (4.29)$$

$$= \frac{_}{1 - \swarrow \mathcal{M}_{n+1} \searrow}. \quad (4.30)$$

The generating function for a (possibly empty) sequence of horizontal segments, each weighted by \tilde{d}_n , is simply $(1 - \tilde{d}_n z)^{-1}$. An up-down pair $\swarrow \cdots \searrow$ from height n to $n + 1$ contributes the weight $\tilde{c}_{n+1} z^2$. We thus arrive at the generating-function recursion

$$\mathcal{M}_n(z) = \frac{(1 - \tilde{d}_n z)^{-1}}{1 - \tilde{c}_n z^2 \mathcal{M}_{n+1}(z) (1 - \tilde{d}_n z)^{-1}} = \frac{1}{1 - \tilde{d}_n z - \tilde{c}_{n+1} z^2 \mathcal{M}_{n+1}(z)}. \quad (4.31)$$

Starting at $n = 0$ and iterating, we find that the generating function $\mathcal{Z}(\tilde{\alpha}, \tilde{\beta}, q, z)$ for Motzkin paths of arbitrary length (and hence the grand-canonical PASEP normalization) is given by the infinite continued fraction

$$\mathcal{Z}(\tilde{\alpha}, \tilde{\beta}, q, z) = \frac{1}{1 - \tilde{d}_0 z - \frac{\tilde{c}_1 z^2}{1 - \tilde{d}_1 z - \frac{\tilde{c}_2 z^2}{1 - \tilde{d}_2 z - \frac{\tilde{c}_3 z^2}{\ddots}}}}, \quad (4.32)$$

where we have dropped the factor h_0 since this does not contribute to any physical quantities. Such a continued fraction containing both z and z^2 terms is usually denoted a *Jacobi continued fraction*, or “J-fraction” for short [15].

Before considering the case of general q let us take $q = 0$ and see how the expression

for the grand canonical normalization, Eq. (2.10), is recovered. We have

$$\mathcal{Z}(\tilde{\alpha}, \tilde{\beta}, 0, z) = \frac{1}{1 - \tilde{d}_0 z - \frac{\tilde{c}_1 z^2}{1 - 2z - \frac{z^2}{1 - 2z - \frac{z^2}{\dots}}}}}, \quad (4.33)$$

where $\tilde{d}_0 = 1/\alpha + 1/\beta$ and $\tilde{c}_1 = 1/\alpha + 1/\beta - 1/(\alpha\beta) = \kappa^2$ when $q = 0$. Note that in this case, the continued fraction is periodic after the first level. That is, in the above notation,

$$\mathcal{M}_n(z) = \frac{1}{1 - 2z - z^2 \mathcal{M}_{n+1}(z)} \quad \forall n \geq 1. \quad (4.34)$$

Hence, we must have that $\mathcal{M}_1(z) = \mathcal{M}_2(z) = \dots$ and hence

$$\mathcal{M}_1(z) [1 - 2z - z^2 \mathcal{M}_1(z)] = 1 \quad (4.35)$$

or

$$\mathcal{M}_1(z) = \frac{1 - 2z - \sqrt{1 - 4z}}{2z^2}, \quad (4.36)$$

which is the generating function familiar from many Catalan counting problems. For $n = 0$, we have

$$\mathcal{Z}(\tilde{\alpha}, \tilde{\beta}, 0, z) = \mathcal{M}_0(z) = \frac{1}{1 - \tilde{d}_0 z - \tilde{c}_1 z^2 \mathcal{M}_1(z)}, \quad (4.37)$$

which coincides with (2.10) when both are expanded and rationalized.

At $q = 0$ the luxury of being able to sum the continued fraction to get equation (4.37) makes the phase structure, which (as previously discussed) is determined by the singularities of $\mathcal{Z}(\tilde{\alpha}, \tilde{\beta}, 0, z)$ in z , immediately apparent. If we are *not* able to easily sum explicitly the continued fraction, as is the case for the PASEP, we can use more indirect methods to determine the singularities. We focus here on the “forward-bias” regime, $q < 1$, in which the continued fraction has a finite radius of convergence in the complex- z plane. In the reverse-bias regime, $q > 1$, the continued fraction is unconditionally divergent, a fact we will interpret physically in Section 7.

We first appeal to Worpitzky’s theorem on the convergence of continued fractions [15, 16] which states that a continued fraction of the form

$$\frac{1}{1 + \frac{a_2}{1 + \frac{a_3}{1 + \frac{a_4}{\dots}}}}} \quad (4.38)$$

converges if the partial numerators a_p satisfy

$$|a_p| < 1/4, \quad p = 2, 3, 4, \dots \quad (4.39)$$

For $\mathcal{Z}(z)$ given by (4.33) this translates to a radius of convergence z_{cr} given by

$$\frac{4\tilde{c}_n z_{cr}^2}{(1 - \tilde{d}_{n-1} z_{cr})(1 - \tilde{d}_n z_{cr})} = 1 \quad \forall n \quad (4.40)$$

and shows that

$$z_{cr} \rightarrow (1 - q)/4 \quad (4.41)$$

as $n \rightarrow \infty$. To decide if this is the dominant singularity, one must also divine the location of any poles in the complex- z plane from the continued fraction (4.32).

The strategy is to examine the n^{th} convergent of the continued fraction, that is, the expression obtained by truncating the continued fraction at the n^{th} level (counting from zero). Denoting this as K_n , we have that

$$K_0 = \frac{1}{1 - \tilde{d}_0 z} , \quad (4.42)$$

$$K_1 = \frac{1}{1 - \tilde{d}_0 z - \frac{\tilde{c}_1 z^2}{1 - \tilde{d}_1 z}} , \quad (4.43)$$

and so on. We observe that the continued fraction (4.33) is given *exactly* by the convergent K_n if $\tilde{c}_{n+1} = 0$. Inspection of (4.26) reveals that this occurs on the special line in the phase diagram given by

$$\tilde{\alpha}\tilde{\beta} = q^{-n} . \quad (4.44)$$

We observe that on such special lines, the matrix C_q decomposes into two blocks: the first is $(n + 1)$ -dimensional, whilst the second does not contribute to the normalisation because only the first elements of the boundary vectors are nonzero. Finite-dimensional representations of the matrix algebra for the PASEP were used prior to the advent of the full solution to study the model along these lines, and to conjecture the phase behaviour elsewhere [8, 9].

To locate the poles of K_n in the complex- z plane, we use the fact [17] that the reciprocal of each convergent K_n can be expressed as

$$(K_n)^{-1} = \frac{A_n}{B_n} \quad (4.45)$$

where A_n and B_n both satisfy the same three-term recurrence

$$A_n(z) = (1 - \tilde{d}_n z)A_{n-1}(z) - \tilde{c}_n z^2 A_{n-2}(z) , \quad (4.46)$$

$$B_n(z) = (1 - \tilde{d}_n z)B_{n-1}(z) - \tilde{c}_n z^2 B_{n-2}(z) , \quad (4.47)$$

but with slightly different initial conditions: $A_{-2} = B_{-1} = 0$ and $A_{-1} = B_0 = 1$. Hence, K_n has poles that coincide with the zeros of $A_n(z)$. These relations for $A_n(z)$ and $B_n(z)$ hold for arbitrary choices of $\tilde{\alpha}$ and $\tilde{\beta}$. Let us now define the function $\mathcal{A}_n(z)$ that is given by $A_n(z)$ for the particular choice $\tilde{\beta} = 1/(q^n \tilde{\alpha})$. That is, the zeros of $\mathcal{A}_n(z)$ give the poles of the PASEP grand-canonical generating function along the line in the phase diagram along which the $(n + 1)$ -dimensional matrix representation is exact.

As a consequence of the recurrence (4.46) the $A_n(z)$ are closely related to the al-Salam-Chihara polynomials [18] and may be written explicitly as

$$A_n(z) = \frac{(\tilde{\alpha}\tilde{\beta}; q)_{n+1} z^{n+1}}{(1-q)^{n+1} \tilde{\alpha}^{n+1}} \sum_{k=0}^{n+1} \frac{(q^{-(n+1)}; q)_k (\tilde{\alpha} e^{i\theta}; q)_k (\tilde{\alpha} e^{-i\theta}; q)_k}{(\tilde{\alpha}\tilde{\beta}; q)_k (q; q)_k} q^k \quad (4.48)$$

where $\cos(\theta) = (1-q)/(2z) - 1$. If we take $\tilde{\beta} = 1/(q^n \tilde{\alpha})$ to obtain $\mathcal{A}_n(z)$ all the terms in the sum in (4.48) will be zero apart from the $(n+1)$ th since they contain a $(1 - \tilde{\alpha}\tilde{\beta}q^n)$ factor in the numerator, which is cancelled only in the last term. Using

$$(\tilde{\alpha} e^{i\theta}; q)_{n+1} (\tilde{\alpha} e^{-i\theta}; q)_{n+1} = \prod_{j=0}^n (1 - 2\tilde{\alpha} q^j \cos(\theta) + \tilde{\alpha}^2 q^{2j}) \quad (4.49)$$

we thus find

$$\mathcal{A}_n(z) = \prod_{k=0}^n \left(1 - \frac{z}{z_k}\right) \quad (4.50)$$

where

$$z_k = \frac{1-q}{\left(1 + \tilde{\alpha} q^k\right) \left(1 + \frac{1}{\tilde{\alpha} q^k}\right)}. \quad (4.51)$$

Equally, we could have taken $\tilde{\alpha} = 1/(q^n \tilde{\beta})$ and obtained the same result with $\tilde{\alpha} \leftrightarrow \tilde{\beta}$. These roots correspond to the reciprocal of the eigenvalues of the finite-dimensional matrices C_q examined in [8, 9] (note, however, that the representation used in those works differs from that used here). This fact can be understood by making the ansatz $A_n(z) = z^n |C_q^{(n)} - \frac{1}{z}|$, where $C_q^{(n)}$ is the submatrix formed by the first n rows and columns of C_q . After substituting into (4.46), one obtains the expression that results from a co-factor expansion along the bottom row in the determinant $|C_q^n - \lambda|$, as long as λ is identified with $\frac{1}{z}$.

We see, then, that the sequence of generating functions $\mathcal{A}_n(z)$ has a truly remarkable property: all poles of $\mathcal{A}_n(z)$ are poles of $\mathcal{A}_m(z)$ where $m > n$. In principle, a completely different set of singularities could have been obtained after truncating at a deeper level. Furthermore, when $q < 1$, $|z_n| < |z_m|$ if $n < m$, and hence all convergents have the same dominant pole, z_0 . Writing this in terms of the original rates α and β gives

$$z_{cr} = \frac{1-q}{2 + \tilde{\alpha} + 1/\tilde{\alpha}} = \frac{\alpha(1-q-\alpha)}{1-q} \quad (4.52)$$

or

$$z_{cr} = \frac{1-q}{2 + \tilde{\beta} + 1/\tilde{\beta}} = \frac{\beta(1-q-\beta)}{1-q}. \quad (4.53)$$

Taking now the number of levels (or, equivalently, the dimensionality of the matrix representation) to infinity, we find that the dominant singularity will always be the smallest of (4.41), (4.52) or (4.53). This observation allows us to recover the reduced

free energies for the PASEP previously calculated in [3,4], and identify the regions of the phase diagram within which they apply:

$$\begin{aligned}
 f &= \ln \left[\frac{1-q}{4} \right], & \text{for } \alpha, \beta > (1-q)/2, \\
 f &= \ln \left[\frac{\alpha(1-q-\alpha)}{1-q} \right], & \text{for } \beta > \alpha, \alpha < (1-q)/2, \\
 f &= \ln \left[\frac{\beta(1-q-\beta)}{1-q} \right], & \text{for } \alpha > \beta, \beta < (1-q)/2.
 \end{aligned} \tag{4.54}$$

As for the ASEP, this phase structure comprises high- and low-density phase and a maximal current phase. The key differences lie in the q -dependent position of the second-order transition line, $\alpha = \beta = (1-q)/2$, and in the subextensive corrections to the free energy, which manifest themselves in the density profile at finite distances from the boundaries [20].

As noted above, this analysis of the PASEP phase behaviour is similar to that based on finite-dimensional matrix representations [8,9]. The main additional benefit of the present approach is that the relationship between the general expression for the normalisation, given through the non-terminating continued fraction (4.32), and the versions that apply only on special lines is clearer. For example, the singularity that arises from non-convergence of the continued fraction, and which governs the maximal-current behaviour, is not detectable by inspection of the finite dimensional matrices. Furthermore, some light is shed on the “continuity arguments” expounded in [8,9] that lead one to extend physical properties found along special lines to regions of the phase diagram, in that each additional level of the continued fraction yields a singularity that is subdominant to all of those present at the previous level. We remark that the fact that the asymptotically dominant singularity is present even in the one-dimensional representation is suggestive of an explanation as to why the phase diagram and currents obtained from mean-field theory coincide with the exact results.

5. Lattice Paths for Non-Zero “Wrong Direction” Removal and Injection Rates γ and δ

As we noted in the introduction it is possible to generalize the PASEP boundary conditions to allow “wrong direction” injection and removal rates. In addition to injection at a rate α at the left boundary particles may also be removed there at a rate γ . Similarly, in addition to removal at a rate β at the right boundary particles may also be injected there at a rate δ .

A tridiagonal representation of D and E with these generalized boundary conditions

still exists for the case of non-zero γ and δ [5] and which can be written as

$$\hat{D}_q = \frac{1}{1-q} \begin{pmatrix} 1 + d_0^\sharp & d_0^\sharp & 0 & \cdots \\ d_0^\flat & 1 + d_1^\sharp & d_1^\sharp & \\ 0 & d_1^\flat & 1 + d_2^\sharp & \ddots \\ \vdots & & \ddots & \ddots \end{pmatrix},$$

$$\hat{E}_q = \frac{1}{1-q} \begin{pmatrix} 1 + e_0^\sharp & e_0^\sharp & 0 & \cdots \\ e_0^\flat & 1 + e_1^\sharp & e_1^\sharp & \\ 0 & e_1^\flat & 1 + e_2^\sharp & \ddots \\ \vdots & & \ddots & \ddots \end{pmatrix}, \quad (5.55)$$

$$\langle \tilde{W}_q | = h_0^{1/2} (1, 0, 0, \dots), \quad | \tilde{V}_q \rangle = h_0^{1/2} (1, 0, 0, \dots)^T, \quad (5.56)$$

where the expressions for d_n^\sharp , d_n^\flat , e_n^\sharp , e_n^\flat (a notation borrowed from [5]) and h_0 are given in the appendix.

We can define $\hat{C}_q = \hat{D}_q + \hat{E}_q$ in an analogous manner to the earlier discussion which leads to a generating function of the form

$$\mathcal{Z}(a, b, c, d, q, z) = \frac{1}{1 - \hat{d}_0 z - \frac{\hat{c}_1 z^2}{1 - \hat{d}_1 z - \frac{\hat{c}_2 z^2}{1 - \hat{d}_2 z - \frac{\hat{c}_3 z^2}{\dots}}}}, \quad (5.57)$$

where the coefficients are now

$$\hat{d}_n = \frac{2 + d_n^\sharp + e_n^\flat}{1 - q},$$

$$\hat{c}_{n+1} = \frac{(d_n^\sharp + e_n^\sharp)(d_n^\flat + e_n^\flat)}{(1 - q)^2}. \quad (5.58)$$

Even with these more complicated coefficients the singularity structure of the generating function is identical to the $\gamma = \delta = 0$ case when $q < 1$. We can still extract poles in order to discern the high- and low-density phases. Explicitly,

$$\hat{c}_{n+1} = \frac{(1 - q^{n-1}abcd)(1 - q^{n+1})(1 - q^n ab)(1 - q^n ac)(1 - q^n ad)(1 - q^n bc)(1 - q^n bd)(1 - q^n cd)}{(1 - q^{2n-1}abcd)(1 - q^{2n}abcd)^2(1 - q^{2n+1}abcd)(1 - q)^2} \quad (5.59)$$

(in which the parameters a , b , c and d are also given in the appendix) so that we can pick up the various poles depending on the zeros of the numerator. For non-zero γ and δ Askey-Wilson polynomials [19] play the role of the al-Salam-Chihara polynomials so in this case the denominators of the convergents are given by

$$A_n(z) = \frac{(ab, ac, ad; q)_{n+1} z^{n+1}}{(1 - q)^{n+1} a^{n+1}} \sum_{k=0}^{n+1} \frac{(q^{-(n+1)}; q)_k (q^n abcd) (a e^{i\theta}; q)_k (a e^{-i\theta}; q)_k}{(ab; q)_k (ac; q)_k (ad; q)_k (q; q)_k} q^k \quad (5.60)$$

where $\cos(\theta) = (1 - q)/(2z) - 1$ as before. If we now choose $q^n ab = 1$, for example, to enforce $\hat{c}_{n+1} = 0$ we find that only the final term in the sum contributes again, resulting in the dominant poles

$$z_{cr} = \frac{1 - q}{2 + a + 1/a} \quad (5.61)$$

or

$$z_{cr} = \frac{1 - q}{2 + b + 1/b} \quad (5.62)$$

depending on the relative size of a and b . The maximal current phase is still observed in a similar manner to the $\gamma = \delta = 0$ case via Worpitzky's theorem but a major difference is that the reverse bias phase is absent when $q > 1$, since the particles can now escape at both ends. Algebraically this is manifested in the reflection symmetry relating the parameters for $q < 1$ and $q > 1$ when γ and δ are non-zero:

$$a, b, c, d, q \rightarrow b^{-1}, a^{-1}, d^{-1}, c^{-1}, q^{-1}. \quad (5.63)$$

We remark that this continued-fraction representation provides a very quick route to the identification of the dominant singularities in the generating function, and therewith the extensive part of the free energy.

6. Correlation Lengths

We have so far restricted our discussion to the normalization itself but it is also possible to extract the correlation lengths, which determine the various sub-phases within the PASEP phase diagram, in a rather straightforward manner. We have seen that the leading singularities of the grand-canonical normalization \mathcal{Z} determine the phase structure of the PASEP and that these can be extracted from the continued fraction representation either directly as poles when the fraction terminates (the high- and low-density phases), or using Worpitzky's theorem (the maximal current phase).

For a chain of length N the one- and two-point density correlation functions for the PASEP may be obtained in terms of the matrices D_q and C_q as

$$\begin{aligned} \langle \tau_i \rangle &= \frac{1}{Z_N} \langle W | C_q^{i-1} D_q C_q^{N-i} | V \rangle, \\ \langle \tau_i \tau_j \rangle &= \frac{1}{Z_N} \langle W | C_q^{i-1} D_q C_q^{j-i-1} D_q C_q^{N-j} | V \rangle. \end{aligned} \quad (6.64)$$

We have already evaluated the thermodynamic limit $N \rightarrow \infty$ of Z_N by picking up the leading singularity in the partial fraction representation. If we switch back to the transfer matrix picture of C_q , the leading singularity of the generating function z_{cr} is just the inverse of the largest eigenvalue of C_q , $\lambda_{cr} = 1/z_{cr}$, which dominates the normalization as

$$\begin{aligned} \langle W | C_q^N | V \rangle &= \sum_{\lambda} \langle W | C_q^N | \lambda \rangle \langle \lambda | V \rangle \\ &= \sum_{\lambda} \langle W | \lambda \rangle \lambda^N \langle \lambda | V \rangle \end{aligned}$$

$$\simeq \text{const. } \lambda_{cr}^N . \quad (6.65)$$

For the two-point function, there is a similar expansion [21]

$$\begin{aligned} & \langle W | C_q^{i-1} D_q C_q^{j-i-1} D_q C_q^{N-j} | V \rangle \\ & \simeq \lambda_{cr}^{N-2} \langle W | \lambda_{cr} \rangle \langle \lambda_{cr} | D_q | \lambda_{cr} \rangle \langle \lambda_{cr} | D_q | \lambda_{cr} \rangle \langle \lambda_{cr} | V \rangle \\ & \quad + \lambda_{cr}^{N-2} \left(\frac{\lambda_{sub}}{\lambda_{cr}} \right)^{i-1} \langle W | \lambda_{sub} \rangle \langle \lambda_{sub} | D_q | \lambda_{cr} \rangle \langle \lambda_{cr} | D_q | \lambda_{cr} \rangle \langle \lambda_{cr} | V \rangle \\ & \quad + \lambda_{cr}^{N-2} \left(\frac{\lambda_{sub}}{\lambda_{cr}} \right)^{j-i-1} \langle W | \lambda_{cr} \rangle \langle \lambda_{cr} | D_q | \lambda_{sub} \rangle \langle \lambda_{sub} | D_q | \lambda_{cr} \rangle \langle \lambda_{cr} | V \rangle \\ & \quad + \lambda_{cr}^{N-2} \left(\frac{\lambda_{sub}}{\lambda_{cr}} \right)^{N-j} \langle W | \lambda_{cr} \rangle \langle \lambda_{cr} | D_q | \lambda_{cr} \rangle \langle \lambda_{cr} | D_q | \lambda_{sub} \rangle \langle \lambda_{sub} | V \rangle , \end{aligned} \quad (6.66)$$

where the second largest eigenvalue λ_{sub} is the inverse of the sub-dominant singularity z_{sub} in the generating function \mathcal{Z} . From this it is clear that the ratio $\lambda_{sub}/\lambda_{cr}$, or alternatively z_{cr}/z_{sub} , determines the correlation length.

If we consider first the high- and low-density phases the sub-dominant singularity is separated from the dominant one and both can be read off directly from the continued fraction representation of \mathcal{Z} . In this case we descend two levels in the continued fraction in order to extract both the dominant and sub-dominant singularities, which means that we impose $\tilde{c}_2 = 0$, i.e., $\tilde{\beta} = 1/(\tilde{\alpha}q)$ or $\tilde{\alpha} = 1/(\tilde{\beta}q)$ depending on the values of the parameters. The generating function then truncates to

$$\begin{aligned} \mathcal{Z}_2(\tilde{\alpha}, \tilde{\beta}, q, z) &= \frac{1}{1 - \tilde{d}_0 z - \frac{\tilde{c}_1 z^2}{1 - \tilde{d}_1 z}} \\ &= \frac{1 - \tilde{d}_1 z}{1 - (\tilde{d}_0 + \tilde{d}_1)z + (\tilde{d}_0 \tilde{d}_1 - \tilde{c}_1)z^2} , \end{aligned} \quad (6.67)$$

which allows us to extract both the dominant singularity z_{cr} and subdominant singularity z_{sub} for various ranges of the parameters $\tilde{\alpha}, \tilde{\beta}, q$. As we have already noted in extracting the normalization from the continued fraction, descending to deeper levels still picks up z_{cr} and z_{sub} as the dominant and sub-dominant pole at every deeper level, in addition to the further sub-leading singularities.

This in turn allows us to classify various sub-phases within the high- and low-density phases which have different behaviours of the correlation length. For example, the low-density phase may be divided into the three sub-phases found in [21]:

(A₁) $\tilde{\alpha}q > 1$, $\tilde{\alpha}q > \tilde{\beta}$:

$$z_{cr} = \frac{1 - q}{(1 + \tilde{\alpha})(1 + \tilde{\alpha}^{-1})} , \quad z_{sub} = \frac{1 - q}{(1 + \tilde{\alpha}q)(1 + (\tilde{\alpha}q)^{-1})} ; \quad (6.68)$$

(A₂) $\tilde{\alpha} > \tilde{\beta} > \tilde{\alpha}q$, $\tilde{\beta} > 1$:

$$z_{cr} = \frac{1 - q}{(1 + \tilde{\alpha})(1 + \tilde{\alpha}^{-1})} , \quad z_{sub} = \frac{1 - q}{(1 + \tilde{\beta})(1 + \tilde{\beta}^{-1})} ; \quad (6.69)$$

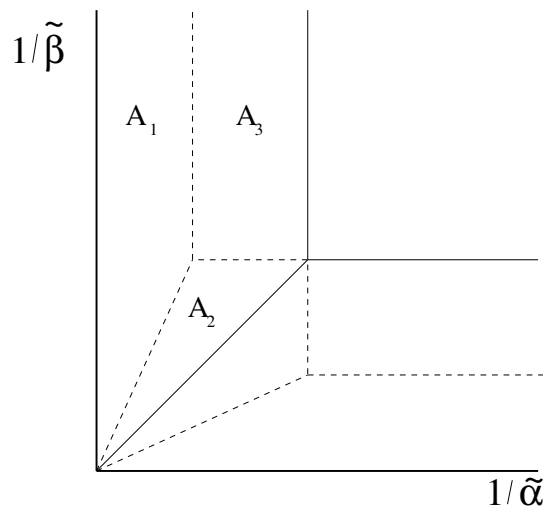


Figure 4. The various sub-phases A_1, A_2, \dots of the PASEP defined by the behaviour of the correlation length are delineated.

(A_3) $\tilde{\alpha} > 1 > \tilde{\alpha}q$, $\tilde{\beta} < 1$:

$$z_{cr} = \frac{1-q}{(1+\tilde{\alpha})(1+\tilde{\alpha}^{-1})}, \quad z_{sub} = \frac{1-q}{4}. \quad (6.70)$$

The z_{sub} values which play a role in the A_1 and A_2 sub-phases are the (sub-dominant) poles of the truncated $\mathcal{Z}_2(\tilde{\alpha}, \tilde{\beta}, q, z)$, whereas in the A_3 sub-phase it is the singularity determined using Worpitzsky's theorem for the full, untruncated \mathcal{Z} . The high-density phase splits in a similar fashion with $\tilde{\alpha}$ and $\tilde{\beta}$ interchanged in the various expressions for z_{cr} and z_{sub} above. In all these sub-phases the correlation functions decay exponentially and the correlation length is given by the log of the ratio of the poles $\xi = (\ln(z_{sub}/z_{cr}))^{-1}$. The phase structure deduced in this manner by considering the singularities of \mathcal{Z} agrees, as it should, with that obtained from considering the integral representation of Z_N in [21] and is shown in figure 4.

7. (Motzkin) Path Transitions

In our earlier work on Dyck path representations of the ASEP normalization it was found that the high- and low-density phases of the ASEP were reflected in bound phases for the lattice paths, whereas the maximal current phase corresponded to an unbound phase. The second-order transition lines of the ASEP corresponded to unbinding transition lines for one of the two lattice paths which described the ASEP normalization and the first-order transition between the high- and low-density phases of the ASEP corresponded to a cooperative transition involving both paths.

The situation for the $q < 1$ phase structure of the PASEP is analogous. In the region of the phase diagram corresponding to the high- and low-density phases of the PASEP predominantly one type of horizontal step is bound to the x -axis, reflecting the majority of particles or holes in the high- and low-density phases of the PASEP. In the

maximal current phase the entropy dominates and paths are unbound. For instance, in the low-density A phases, indicated in figure 4, the horizontal on-axis steps weighted by $1 + \tilde{\alpha}$ will make a greater contribution to the partition function than those weighted by $1 + \tilde{\beta}$ and so will dominate the sum. The reverse is true in the high-density phase where the steps weighted by $1 + \tilde{\beta}$ dominate.

The non-trivial terms in the weights of steps at height n are proportional to q^n so these steps do not contribute to the energy as $N \rightarrow \infty$ when $q < 1$, but only entropically. It is therefore not surprising that for $q < 1$ the PASEP phase diagram is essentially identical to the ASEP, with only the position of the transition lines changing as q is varied. It is interesting to inquire about the nature of the paths contributing to the partition function for $q > 1$. The expression for Z_N in this reverse bias phase was calculated in [4],

$$Z_N \sim A(\tilde{\alpha}, \tilde{\beta}; q) (q^{-1}\tilde{\alpha}\tilde{\beta}, 1/\tilde{\alpha}\tilde{\beta}; q^{-1})_\infty \left(\frac{\sqrt{\tilde{\alpha}\tilde{\beta}}}{q-1} \right)^N q^{\frac{1}{4}N^2}, \quad (7.71)$$

where

$$A(\tilde{\alpha}, \tilde{\beta}; q) = \sqrt{\frac{\pi}{\ln q}} \exp \left[M(q) + \frac{(\ln \tilde{\beta}/\tilde{\alpha})^2}{4 \ln q} \right], \quad (7.72)$$

and

$$M(q) \simeq - \sum_{k=1}^{\infty} \frac{1}{k} \frac{1}{q^k - 1}. \quad (7.73)$$

The most interesting feature of (7.71) is that one now sees an area-like behaviour emerging, whereby $Z_N \sim q^{\frac{1}{4}N^2}$.

To see how such two-dimensional behaviour emerges from a model of one-dimensional paths when $q > 1$ consider a tent-shaped path contributing to Z_N with $N/2$ upward steps followed by $N/2$ downward steps. This has a weight

$$\frac{(\tilde{\alpha}\tilde{\beta}; q)_{N/2} (q; q)_{N/2}}{(q-1)^N}, \quad (7.74)$$

which has a leading term of the form

$$\frac{(\tilde{\alpha}\tilde{\beta} - 1)(\tilde{\alpha}\tilde{\beta})^{\frac{N}{2}-1} q^{\frac{N^2}{4}}}{(q-1)^N}. \quad (7.75)$$

The reverse bias expression for Z_N in (7.71) displays exactly this behaviour. With a slight rewriting of the second factor,

$$Z_N \sim A(\tilde{\alpha}, \tilde{\beta}; q) (q^{-1}\tilde{\alpha}\tilde{\beta}, 1/q\tilde{\alpha}\tilde{\beta}; q^{-1})_\infty \left(\frac{\tilde{\alpha}\tilde{\beta} - 1}{\tilde{\alpha}\tilde{\beta}} \right) \left(\frac{\sqrt{\tilde{\alpha}\tilde{\beta}}}{q-1} \right)^N q^{\frac{1}{4}N^2}, \quad (7.76)$$

which matches the behaviour of (7.75) coming from a ‘‘tent’’ path. Heuristically this makes sense since paths which gain in altitude as quickly as possible will donate the highest powers of q to Z_N and dominate when $q > 1$.

This change in behaviour at $q > 1$ to an area-like scaling is thus interpreted in the lattice path picture as an inflation transition, where the fluctuating path becomes the boundary of an inflated vesicle (with particular edge weights favouring a speedy ascent) pinned at its ends to the horizontal axis. The matrices D_q and E_q initially denoted the presence or absence of particles on a particular site in the original matrix product ansatz. We can associate an up-step and one colour of horizontal step in a path with, say, the presence of a particle in the original PASEP steady state. Looking at the form of the leading contribution to Z_N when $q > 1$, namely $N/2$ up-steps followed by $N/2$ down-steps, we can see that this corresponds to a half-filled lattice, which has also been observed in simulations of the reverse bias phase and heuristically derived using particle/hole symmetry arguments [4].

The form of equation (7.71) is reminiscent of the partition function for inflated lattice vesicles with a fixed perimeter discussed in [22]. If one models a two-dimensional vesicle with a convex polygon of perimeter $2N$ on a square lattice then the partition function is given by

$$Z_N(q) \sim \frac{(1 + O(\rho^N))}{(q^{-1}; q^{-1})_\infty^4} \sum_{k=1}^{N-1} q^{k(N-k)}, \quad (7.77)$$

where each component square making up the polygon has a weight q and $\rho < 1$. The summation arises from rectangles and may be extended to run from $\pm\infty$ with an error of $O(q^{-\frac{N^2}{4}})$ and the prefactor can be thought of as arising from nibbling off the corners of the rectangles with Ferrers diagrams as described in [22]. In the case of the PASEP the expression for Z_N when $q > 1$ is suggestive of a similar interpretation; the leading “tent” term is decorated with nibbled edges from the fluctuations.

8. The Case $q = 1$

The expression for Z_N may also be evaluated in the case of the symmetric simple exclusion process (SSEP) when $q = 1$. If we introduce some more standard notation, this time for q -numbers,

$$[n]_q = \frac{1 - q^n}{1 - q} = 1 + q + \dots + q^{n-1}, \quad (8.78)$$

(with $[n]_q = 0$ for $n \leq 0$) we can rewrite the Motzkin-path weights as

$$\begin{aligned} \tilde{d}_n &= 2[n]_q + \left(\frac{1}{\alpha} + \frac{1}{\beta}\right) q^n, \\ \tilde{c}_n &= [n]_q \left([n-1]_q + \left(\frac{1}{\alpha} + \frac{1}{\beta}\right) q^{n-1} - \frac{(1-q)q^{n-1}}{\alpha\beta} \right), \end{aligned} \quad (8.79)$$

or, splitting the horizontal weights into two types of steps again in order to make the correspondence with bicoloured Motzkin paths explicit,

$$\begin{aligned} \tilde{d}_{n,1} &= [n]_q + \frac{q^n}{\alpha}, \\ \tilde{d}_{n,2} &= [n]_q + \frac{q^n}{\beta}. \end{aligned} \quad (8.80)$$

The q -integers become normal integers when $q = 1$, so the weights at $q = 1$ are given by

$$\begin{aligned}\tilde{d}_{n,1} &= n + \frac{1}{\alpha}, \\ \tilde{d}_{n,2} &= n + \frac{1}{\beta}, \\ \tilde{c}_n &= n \left(n - 1 + \frac{1}{\alpha} + \frac{1}{\beta} \right),\end{aligned}\tag{8.81}$$

which simplify even further when $\alpha = \beta = 1$ to $n + 1$ and $n(n + 1)$. This gives

$$\mathcal{Z}(1, 1, 1, z) = \frac{1}{1 - 2z - \frac{2z^2}{1 - 4z - \frac{2 \times 3z^2}{1 - 6z - \frac{3 \times 4z^2}{\dots}}}}},\tag{8.82}$$

which can be seen to be a continued fraction expansion for the divergent power series

$$\mathcal{Z} = \sum_{N=0}^{\infty} (N + 1)! z^N,\tag{8.83}$$

so $Z_N = (N + 1)!$ in this case. A similar expansion exists for general α and β and gives Z_N as the ratio of two Gamma functions,

$$Z_N = \frac{\Gamma(\lambda + N + 1)}{\Gamma(\lambda + 1)}\tag{8.84}$$

where $\lambda = \frac{1}{\alpha} + \frac{1}{\beta} - 1$. This agrees with a direct calculation in [5]. Using Stirling's approximation for the Gamma functions, and remembering that λ is of $O(1)$ we see that $\ln Z_N \sim N \ln N$ so $Z_N \sim e^{N \ln N}$ at $q = 1$, intermediate between the linear behaviour for $q < 1$ and the area law behaviour when $q > 1$.

9. The Case $q^{n+1} = 1$

The continued fraction representation of \mathcal{Z} will also terminate when $q^{n+1} = 1$. These values of q have recently proved of interest for the Bethe Ansatz approach to the open XXZ spin chain with non-diagonal boundary conditions [23–25]. The Hamiltonian of the XXZ spin chain is equivalent (up to a unitary transformation) to the transfer matrix of the PASEP. If we denote the expression for $A_n(z)$ when $q^{n+1} = 1$ by $\tilde{\mathcal{A}}_n(z)$ the sum in (4.48) truncates to two terms

$$\tilde{\mathcal{A}}_n(z) = \frac{z^{n+1}}{(1 - q)^{n+1} \tilde{\alpha}^{n+1}} \left((\tilde{\alpha}\tilde{\beta}; q)_{n+1} - (\tilde{\alpha}e^{i\theta}; q)_{n+1} (\tilde{\alpha}e^{-i\theta}; q)_{n+1} \right)\tag{9.85}$$

where we have used a limiting procedure

$$\lim_{\epsilon \rightarrow 0} \frac{(q^{-n+1}; q)_{n+1}}{(q; q)_{n+1}} = \lim_{\epsilon \rightarrow 0} (-1)^{n+1} q^{-(n+1)(n+2)/2} = -1\tag{9.86}$$

with $q = \exp(\epsilon + 2\pi im/(n + 1))$ to handle the indeterminate final term [26]. Noting that $(\tilde{\alpha}e^{i\theta}, q)_{n+1} = (1 - \tilde{\alpha}^{n+1}e^{i(n+1)\theta})$ when $q^{n+1} = 1$ this can be written as

$$\tilde{\mathcal{A}}_n(z) = \frac{z^{n+1}}{(1 - q)^{n+1}} \left(e^{i(n+1)\theta} + e^{-i(n+1)\theta} - (\tilde{\alpha}^{n+1} + \tilde{\beta}^{n+1}) \right)\tag{9.87}$$

and we find that the zeros of $\tilde{\mathcal{A}}_n(z)$ are given by

$$z_k = \frac{1 - q}{(1 + rq^k)(1 + \frac{1}{rq^k})} \quad (9.88)$$

where r is the root with smaller argument of

$$r^{n+1} = \frac{(\tilde{\alpha}^{n+1} + \tilde{\beta}^{n+1})}{2} + \sqrt{\frac{(\tilde{\alpha}^{n+1} + \tilde{\beta}^{n+1})^2}{4} - 1} \quad (9.89)$$

or

$$r^{-(n+1)} = \frac{(\tilde{\alpha}^{n+1} + \tilde{\beta}^{n+1})}{2} - \sqrt{\frac{(\tilde{\alpha}^{n+1} + \tilde{\beta}^{n+1})^2}{4} - 1}. \quad (9.90)$$

It is interesting that the overall structure of the roots remain similar to that observed when $\tilde{\alpha} = 1/(q^n \tilde{\beta})$, but one no longer has a dominant pole appearing at first order and remaining.

10. Conclusions

We have shown that the matrix $C_q = D_q + E_q$ in a particular tridiagonal representation of the PASEP algebra can be interpreted as the transfer matrix for weighted Motzkin paths, with two colours of horizontal steps. Writing the generating function for these paths as a continued fraction allowed a succinct derivation of the thermodynamic limit of the normalization of the PASEP in its various phases. In particular it allowed calculations without explicitly summing the generating function in closed form, which was possible (or at any rate, easy to perform) only in the $q = 0$ case. Consideration of the sub-leading singularities in the continued fraction also allowed the determination of the correlation length in the high- and low-density phases.

A further interesting feature of the continued fraction representation of the generating function was that it made clear how the finite-dimensional representations of the PASEP algebra, valid only along special lines in the phase diagram, related to the general, infinite-dimensional solution via truncation. The unusual structure of the poles of the convergents of the continued fraction along these special lines was highlighted, with lower order poles remaining present as the order of the convergent increased and the dominant pole (for the high- and low-density phases) already being present at zeroth order. The presence of the maximal current phase, on the other hand, was deduced from the continued fraction representation by using Worpitzky's theorem.

The phase transitions of the PASEP can be identified with transitions in the lattice path model. When $q < 1$ there are similar unbinding transitions to those seen in the Dyck path model for the ASEP, with bound states corresponding to the high- and low-density phases of the PASEP and an unbound phase corresponding to the maximal current phase. For the reverse bias phase of the PASEP when $q > 1$ the lattice path model was seen to be in an inflated phase and the leading contribution to the lattice path partition function was identified with a half-filled state in the PASEP.

Interestingly, bicoloured Motzkin paths play a major role in various combinatorial bijections and the ASEP and PASEP have recently been investigated for their combinatorial interest [27–31]. One common theme has been the appearance of various well-known combinatorial weights as special cases for the (P)ASEP normalization which can be related to known results in the enumeration of permutations and other combinatorial objects. The approach in [29] in particular is rather similar to that espoused here, namely going directly to a matrix representation for D and E and seeking a combinatorial interpretation (although the principal focus in [29] was on a different representation and permutation tableaux).

It would be an interesting exercise to relate the phase transitions discussed here for Motzkin paths and the related phase structure of the PASEP to conformational transitions in other (weighted) combinatorial objects such as parallelogram polyominoes, binary trees and the permutation tableau of [29]. It would also be worthwhile to relate the lattice path picture to discussions of the large deviation functional of the (P)ASEP, such as that in [32], where the appearance of a combination of a Brownian excursion and a Brownian walk in the discussion is strongly suggestive of a polyomino bijection from the Motzkin paths here.

11. Acknowledgements

This work was partially supported by the EU RTN-Network ‘ENRAGE’: *Random Geometry and Random Matrices: From Quantum Gravity to Econophysics* under grant No. MRTN-CT-2004-005616.

Appendix A. Parameters Appearing in the Tridiagonal Matrix Representation for $\gamma, \delta \neq 0$

When all four boundary rates, α , β , γ and δ are nonzero, the tridiagonal D and E matrices (5.55) contain a number of parameters. These are

$$\begin{aligned}
 d_n^\sharp &= \frac{q^{n-1}}{(1 - q^{2n-2}abcd)(1 - q^{2n}abcd)} \\
 &\quad \times [bd(a+c) + (b+d)q - abcd(b+d)q^{n-1} - \{bd(a+c) + abcd(b+d)\}q^n \\
 &\quad - bd(a+c)q^{n+1} + ab^2cd^2(a+c)q^{2n-1} + abcd(b+d)q^{2n}] , \\
 e_n^\sharp &= \frac{q^{n-1}}{(1 - q^{2n-2}abcd)(1 - q^{2n}abcd)} \\
 &\quad \times [ac(b+d) + (a+c)q - abcd(a+c)q^{n-1} - \{ac(b+d) + abcd(a+c)\}q^n \\
 &\quad - ac(b+d)q^{n+1} + a^2bc^2d(b+d)q^{2n-1} + abcd(a+c)q^{2n}] , \\
 d_n^\flat &= \frac{1}{1 - q^n ac} \mathcal{A}_n , & e_n^\sharp &= -\frac{q^n ac}{1 - q^n ac} \mathcal{A}_n , \\
 d_n^\flat &= -\frac{q^n bd}{1 - q^n bd} \mathcal{A}_n , & e_n^\flat &= \frac{1}{1 - q^n bd} \mathcal{A}_n ,
 \end{aligned}$$

which involve the further parameters

$$\begin{aligned}
 a &= \frac{1}{2\alpha} \left[(1 - q - \alpha + \gamma) + \sqrt{(1 - q - \alpha + \gamma)^2 + 4\alpha\gamma} \right], \\
 b &= \frac{1}{2\beta} \left[(1 - q - \beta + \delta) + \sqrt{(1 - q - \beta + \delta)^2 + 4\beta\delta} \right], \\
 c &= \frac{1}{2\alpha} \left[(1 - q - \alpha + \gamma) - \sqrt{(1 - q - \alpha + \gamma)^2 + 4\alpha\gamma} \right], \\
 d &= \frac{1}{2\beta} \left[(1 - q - \beta + \delta) - \sqrt{(1 - q - \beta + \delta)^2 + 4\beta\delta} \right] \\
 \mathcal{A}_n &= \left[\frac{(1-q^{n-1}abcd)(1-q^{n+1})(1-q^n ab)(1-q^n ac)(1-q^n ad)(1-q^n bc)(1-q^n bd)(1-q^n cd)}{(1-q^{2n-1}abcd)(1-q^{2n}abcd)^2(1-q^{2n+1}abcd)} \right]^{1/2}.
 \end{aligned}$$

Finally, the constant appearing in (5.56) is

$$h_0 = \frac{(abcd; q)_\infty}{(q, ab, ac, ad, bc, bd, cd; q)_\infty}. \tag{A.1}$$

- [1] B. Derrida, M. R. Evans, V. Hakim and V. Pasquier, *J. Phys. A: Math. Gen.* **26**, 1493 (1993).
- [2] R. A. Blythe, and M. R. Evans, *J. Phys. A: Math. Theor.* **40**, R333 (2004).
- [3] T. Sasamoto, *J. Phys. A: Math. Gen.* **32**, 7109 (1999).
- [4] R. A. Blythe, M. R. Evans, F. Colaiori and F. H. L. Essler, *J. Phys. A: Math. Gen.* **33**, 2313 (2000).
- [5] M. Uchiyama, T. Sasamoto and M. Wadati, *J. Phys. A: Math. Gen.* **37**, 4985 (2004).
- [6] R. A. Blythe, W. Janke, D. A. Johnston and R. Kenna, *J. Stat. Mech. : Theor. Exp.* P06001 (2004).
- [7] R. A. Blythe, W. Janke, D. A. Johnston and R. Kenna, *J. Stat. Mech. : Theor. Exp.* P10007 (2004).
- [8] K. Mallick and S. Sandow *J. Phys. A: Math. Gen* **30**, 4513 (1997).
- [9] F. H. Jafarpour *J. Phys. A: Math. Gen* **33**, 1797 (2000).
- [10] H. S. Wilf, *Generatingfunctionology* (3rd edition, A K Peters, Wellesley, MA, 2006).
- [11] R. A. Blythe and M. R. Evans, *Phys. Rev. Lett.* **89**, 080601 (2002).
- [12] R. Brak and J. Essam, *J. Phys. A: Math. Gen.* **37**, 4183 (2004).
- [13] R. Brak, J. de Gier and V. Rittenberg, *J. Phys. A: Math. Gen.* **37**, 4303 (2004).
- [14] P. Flajolet, *Discr. Math.* **32**, 125 (1982).
- [15] H. S. Wall, *Analytic Theory of Continued Fractions* (van Nostrand, Princeton, 1948).
- [16] E. J. Janse van Rensburg, *The Statistical Mechanics of Interacting Walks, Polygons, Animals and Vesicles* (Oxford University Press, Oxford, 2000).
- [17] G. E. Andrews, R. Askey and R. Roy, *Special Functions* (Cambridge University Press, Cambridge, 2000).
- [18] W. A. Al-Salam and T. S. Chihara, *SIAM Journal of Mathematical Analysis* **7**, 16 (1976).
- [19] R. A. Askey and J. A. Wilson, *Mem. Am. Math. Soc.* **54**, 319 (1985).
- [20] T. Sasamoto, *J. Phys. Soc. Jpn* **69**, 1055 (2000).
- [21] M. Uchiyama and M. Wadati, *J. Nonlin. Math. Phys.* **12**, 676 (2005).
- [22] T. Prellberg and A. L. Owczarek, *Commun. Math. Phys.* **201**, 493 (1999).
- [23] R. Murgan, R. I. Nepomechie and C. Shi, *J. Stat. Mech. : Theor. Exp.*, P08006 (2006).
- [24] J. de Gier and F. H. L. Essler, *Phys. Rev. Lett.*, **95**, 240601 (2005).
- [25] J. de Gier and F. H. L. Essler, *J. Phys. A: Math. Gen.*, **41**, 485002 (2008).
- [26] V. Spridinov and A. Zhedanov, *Duke Math. J.* **89**, 283 (1997).
- [27] R. Brak, S. Corteel, A. Rechnitzer and J. Essam, *A combinatorial derivation of the PASEP algebra*, FPSAC2005 (2005).

- [28] S. Corteel and L. K. Williams, *Int. Math. Res. Not.*, rnm055 (2007).
- [29] S. Corteel and L. K. Williams, *Tableaux combinatorics for the asymmetric exclusion process*, *Adv. in App. Maths.*, to appear.
- [30] E. Duchi and G. Schaeffer, *Journal of Combinatorial Theory, Series A*, **110(1)**, 1 (2005).
- [31] E. Duchi and G. Schaeffer, *A combinatorial approach to jumping particles: the parallel TASEP*, *FPSAC2005* (2005).
- [32] B. Derrida, C. Enaud and J. L. Lebowitz, *J. Stat. Phys.* **115**, 365 (2004).